Fabrication and Drug Release Study of Double-Layered Microparticles of Various Sizes

WEI LI LEE,[1] YI CHUAN SEH,[1] EFFENDI WIDJAJA,[2] HAN CHUNG CHONG,[3] NGUAN SOON TAN,[3] SAY CHYE JOACHIM LOO[1]

[1]School of Materials Science and Engineering, Nanyang Technological University, Singapore 639798, Singapore

[2]Process Science and Modeling, Institute of Chemical and Engineering Sciences, Jurong Island, Singapore 627833, Singapore

[3]School of Biological Sciences, Nanyang Technological University, Singapore 637551, Singapore

Received 30 January 2012; revised 27 March 2012; accepted 24 April 2012

Published online 9 May 2012 in Wiley Online Library (wileyonlinelibrary.com). DOI 10.1002/jps.23191

ABSTRACT: Double-layered microparticles, composed of poly(D,L-lactide-*co*-glycolide) (50:50) (PLGA) core and poly(L-lactide) (PLLA) shell, of controllable sizes ranging from several hundred microns to few microns were fabricated using a one-step solvent evaporation method. Metoclopramide monohydrochloride monohydrate (MCA), a hydrophilic drug, was selectively localized in the PLGA core. To achieve the double-layered particles of size approximately 2 μm, the process parameters were carefully manipulated to extend the phase separation time by increasing oil-to-water ratio and saturating the surrounding aqueous phase with solvent. Subsequently, the drug release profiles of the double-layered particles of various sizes were studied. Increased particle size resulted in faster degradation of polymers because of autocatalysis, accelerating the release rate of MCA. Interestingly, the effect of degradation rates, affected by particle sizes, on drug release was insignificant when the particle size was drastically reduced to 2–20 μm in the investigated double-layered particles. This understanding would provide critical insights into how the controllable formation and unique drug release profiles of double-layered particles of various sizes can be achieved. © 2012 Wiley Periodicals, Inc. and the American Pharmacists Association J Pharm Sci 101:2787–2797, 2012

Keywords: biodegradable polymers; controlled release; microparticles; multilayers; particle size; polymeric drug delivery systems; solvent evaporation

INTRODUCTION

Over the past few decades, biodegradable microparticles of poly(D,L-lactide-*co*-glycolide) (PLGA) and poly(lactide) (PLA) have been extensively investigated for drug delivery.[1,2] However, monolithic particle-based drug delivery system inherently shows a high initial "burst" caused by the rapid release of the drug particles trapped on or located near the surface.[3] This burst release is detrimental, especially for drugs with a narrow therapeutic window and high toxicity. In addition, hydrophilic drugs have low encapsulation efficiency in single-layered particles composed primarily of hydrophobic polymers, such as PLGA and PLA.[4] To alleviate these problems, multiparticulate drug delivery systems that comprise a polymer shell surrounding one or many micron-sized particulates have been employed.[5–13] The outer layer in this multiparticulate structure acts as a rate-limiting membrane for diffusion of drugs localized in the cores. Schoubben et al.[14] reported that microencapsulating protein-loaded particles within PLGA microparticles allow for the structural integrity of the protein to be maintained, while at the same time reducing initial burst release. Shi et al.[7] also demonstrated a sustained release of bovine serum albumin and cyclosporine A from poly(ortho ester)–PLGA double-layered microparticles.

Although the drug release study of double-layered microparticles has been established, there has been no report on the effect of sizes of multilayered composite microparticles on drug release kinetics and profiles. Particles size could critically influence several determinants associated with device administration and drug release rates. For example, particle sizes ranging from 1 to 10 μm would allow for uptake by antigen-presenting cells such as macrophages.[15] Optimizing particle size can also enhance the

Correspondence to: Say Chye Joachim Loo (Telephone: +65-6790-4603; Fax: +65-6790-9081; E-mail: joachimloo@ntu.edu.sg)

Journal of Pharmaceutical Sciences, Vol. 101, 2787–2797 (2012)

intratumoral or pulmonary delivery.[16,17] Microparticles, especially in the range between 5 and 150 μm, are of much interest for drug delivery depots as they are large enough to be localized at the injection site while administered through a relatively small gauge hypodermic needle.[18] In addition, particle sizes not only affect the diffusion distance of the drug but also the mass transport of acidic degradation products, and consequently, rate of hydrolytic degradation of particles.[19] As such, there is an increasing field of interest to understand how different sizes of double-layered microparticles can influence the degradation behaviors and drug release profiles.

Although previous studies largely revolved around producing larger micron-sized particulate drug delivery systems with various internal morphologies,[20,21] the objective of this paper is therefore to report on the fabrication of double-layered particles (1–10 μm) composed of PLGA (50:50) core and poly(L-lactide) (PLLA) shell through a one-step solvent evaporation technique. The novelty of this paper describes how certain process parameters would require tweaking to produce small-sized particles of double-layered structure. Subsequently, this paper will report how the drug release profiles of double-layered microparticles are altered when particle size is reduced from several hundred microns to few microns. The model drug used in this study was hydrophilic metoclopramide monohydrochloride monohydrate (MCA), and would be localized in the PLGA core, whereas the hydrophobic PLLA shell can serve as a rate-controlling layer for the release of MCA. As a therapeutic agent, MCA can be used to prevent postoperative nausea or treat patients with diabetic gastroparesis. MCA is also used as a radiosensitizing agent in the treatment of non-small-cell lung carcinoma.[22]

6% theoretical

MATERIALS AND METHODS

Materials

Poly(L-lactide) [intrinsic viscosity (IV): 2.38; Bio Invigor (Taiwan)], PLGA (50:50) (IV: 1.18; Bio Invigor (Taiwan)), and poly(vinyl alcohol) (PVA) (molecular weight: 30–70 kDa, Sigma–Aldrich (Singapore)) were used. MCA, laser grade coumarin-6, and rhodamine 6G fluorescent dyes were purchased from Sigma –Aldrich (Singapore). Solvents including dichloromethane (DCM), tetrahydrofuran (THF), and chloroform were purchased from Tedia Company, Inc. (USA). Phosphate-buffered saline (PBS) at pH 7.4 was from OHME (Singapore). All chemicals and solvents were used as received.

Fabrication of Non-Drug and Drug-Loaded Microparticles

Fabrication of PLLA/PLGA microparticles was prepared through an oil-in-water (o/w) emulsion solvent evaporation method.[20,23,24] Briefly, a polymer solution (6%, w/v) consisting of 0.2 g PLLA and 0.1 g PLGA dissolved in 5 mL DCM was first prepared. The resultant polymer solution was then poured into the PVA aqueous solution and emulsified with an overhead stirrer (Calframo BDC 1850-220) at room temperature (25°C). The microparticles formed were collected by centrifugation, washed with deionized water, lyophilized, and stored in a desiccator for subsequent characterization. Table 1 summarizes the process parameters that were altered for the formation of non-drug-loaded PLLA/PLGA microparticles of various sizes.

MCA-loaded double-layered PLLA/PLGA microparticles were produced through a water-in-oil-in-water (w/o/w) double-emulsion solvent evaporation method.[11] The polymers (0.2 g PLLA and 0.1 g PLGA, 6%, w/v) were dissolved in DCM, and the drug (20%, w/w) dissolved in 0.1 mL deionized water was prepared separately. Subsequently, both solutions were mixed and subjected to ultrasonication for 30 s using an ultrasonic processor (Sonic Vibra-Cell VC 130) to form the primary w/o emulsion, after which, the primary emulsion was then added into the PVA aqueous solution containing NaCl (1%, w/v), forming the w/o/w emulsion. It is generally believed that the addition of NaCl to the external aqueous phase (through the built up of osmotic pressure) reduces the loss of drug to the external aqueous phase and forms a dense surface.[25,26] MCA-loaded microparticles of different sizes were then prepared, in a similar manner, whereby the stirring speed and PVA concentration were adjusted accordingly. The final production

Table 1. Parameters Used to Fabricate the Non-Drug-Loaded Composite PLLA/PLGA Microparticles of Various Sizes

Particle Size (μm)	Stirring Speed (rpm)	PVA Concentration in External Aqueous Phase (%, w/v)	Oil-to-Water Ratio	Remarks
276 ± 58.5	350	0.5	0.02	–
18.3 ± 4.8	2000	6	0.02	–
2.3 ± 0.8	2000	6	0.1	1 mL DCM added into PVA solution; coumarin-6 and rhodamine 6G added into polymer solution (1%, w/w) for confocal laser scanning characterization purpose.

Table 2. Parameters Used to Fabricate the MCA-Loaded PLLA/PLGA Microparticles of Various Sizes

Particle Size (μm)	Stirring Speed (rpm)	PVA Concentration in External Aqueous Phase (%, w/v)	Oil-to-Water Ratio	Remarks
286.5 ± 63.2	350	0.5	0.02	–
68.4 ± 24.7	2000	2	0.02	–
17.6 ± 6.5	2000	6	0.02	–
2.2 ± 0.9	2000	6	0.1	1 mL DCM added into PVA solution.

yield for each batch was about 90%. Table 2 summarizes the process parameters used for the formation of MCA-loaded PLLA/PLGA microparticles of various sizes.

Characterization

Scanning Electron Microscopy

The exterior and internal morphologies of the microparticles were viewed using scanning electron microscopy (SEM) (Jeol JSM-6360A, Tokyo, Japan) at 5 kV. Prior to analysis, the samples were first mounted onto a metal stub and submerged in liquid nitrogen before chopping them with a razor blade. Samples were subsequently coated with gold using a sputter coater (SPI-Module). Ten microparticles from each independent batch (at least three of them) for each particle type were randomly chosen to be viewed under the SEM. As particle morphologies were found to be consistent for a particular particle group type, only one representative SEM image is shown. Particle size (in diameter) analysis was performed on the SEM images using the ImageJ software (National Institutes of Health, USA).

Raman Mapping

The polymer and drug distribution within the microparticles were verified through Raman mapping. Raman mapping (point-by-point) measurements on cross-sectioned microparticles were conducted on an area of $300 \times 150\,\mu m$ with a step size of 5 μm in both the x and y directions using a Raman microscope (In-Via Reflex, Renishaw, UK) coupled with a CCD array detector (576×384 pixels) and a Leica microscope. The sample was irradiated using a 785 nm near-infrared diode laser, and the backscattered light was collected by a 50× objective lens. The band target entropy minimization (BTEM) algorithm was devised to reconstruct the spectral estimates of each pure component using the collected Raman mapping data,[27] following which, the spatial distribution of each underlying constituents was generated.

Confocal Laser Scanning Microscopy

Particles loaded with dyes (i.e., coumarin-6 and rhodamine 6G, without suspending particles in a medium) were first placed onto a glass slide and subsequently covered with a cover slip. For coumarin-6 (green dye), the excitation peak was centered at 488 nm, with an emission peak wavelength of 509 nm. For rhodamine 6G (red dye), the excitation peak was centered at 552 nm, with an emission peak wavelength of 575 nm. Images were acquired using an LSM710 confocal microscope (Carl Zeiss, Germany), with 63×/1.40 oil objectives and AxioCan MRm camera (Carl Zeiss) and analyzed using ZEN 2011 software.

Focused Ion Beam

Cross-sections of particles (smaller than 10 μm) were prepared and imaged using focused ion beam (FIB) microscopy (FEI Nova Nanolab 600i). The particles were first mounted onto a lacey copper grid. A Ga^+ ion beam with 30 keV with a beam current of 26 pA was used for milling the target particles. The samples were then imaged by the secondary electrons formed during milling.

Field-Emission SEM Fitted with a Transmission Electron Detector

The particles were first suspended in ethanol and few drops of suspension were subsequently deposited onto a continuous copper grid. The particles were viewed under Jeol JSM-7600F field-emission SEM (FESEM) fitted with a transmission electron detector (TED) at an accelerating voltage of 30 kV.

Drug Encapsulation Efficiency

Encapsulation efficiency is calculated by dividing the actual drug loading with theoretical drug loading within the microparticles. For the determination of hydrophilic MCA loading, 10 mg of microparticles ($n = 3$) were first dissolved in 1 mL of DCM, followed by the addition of deionized water (10 mL) to extract MCA. Ultraviolet–visible (UV–Vis) spectrophotometer (Shimadzu UV-2501, Japan) was used to determine the drug concentration at the wavelength of 309 nm.

Hydrolytic Degradation

Microparticles (50 mg) were placed, in triplicate, in vials containing 30 mL of PBS (pH 7.4) for each time point. *In vitro* hydrolytic degradation of microparticles was performed in a shaking incubator at 37°C.

Microparticles were removed from the vials at predetermined time points.

Molecular Weight

Size-exclusion chromatography (SEC) (Agilent 1100 Series LC System, Germany) was used to determine the molecular weight of each of the samples. The polymers in the double-layered microparticles were separated by the THF dissolution method, where PLGA is soluble in THF, while PLLA is not.[11] Microparticles (8 mg) were initially immersed in 1 mL of THF under mild agitation in order to dissolve the PLGA constituent. The PLLA remnants and PLGA solution were subsequently separated by centrifugation. Afterward, the oven-dried PLGA and PLLA dissolved separately in 1 mL of chloroform were tested with SEC.

Thermal Analysis

Thermal analysis of the microparticles was performed on a modulated differential scanning calorimetry (MDSC™) (DSC 2920, TA Instruments, USA). Approximately 5 mg of microparticles was first heated from −40°C to 200°C, subsequently cooled to −40°C, and lastly reheated to 200°C, all steps were conducted at a rate of $5^{\circ}C \cdot min^{-1}$. Thermograms were analyzed using TA universal analyzer software for the determination of glass transition temperature (T_g).

Drug Release Study

MCA-loaded microparticles (5 mg) placed in vials containing 5 mL of PBS ($n = 3$) were incubated at 37°C in a shaking incubator. One milliliter of medium was removed from each vial at predetermined time intervals, and was analyzed using a UV–Vis spectrophotometer at 309 nm. Each sample was replenished with fresh PBS after removing for analysis.

Statistical Analysis

Data from different sets of particles were compared by unpaired Student's *t*-test and the one-way analysis of variance analysis coupled with Tukey's multiple comparison tests. Statistically significant differences were verified when $p \leq 0.05$.

RESULTS AND DISCUSSION

Fabrication of Non-Drug-Loaded Double-Layered Particles

A reference set (Table 1) of large-sized double-layered microparticles was initially fabricated before proceeding with the manipulation of process parameters to reduce particle size. The SEM micrographs of the reference double-layered microparticles are shown in Figures 1a and 1b, of particle size 276 ± 58.5 μm and average shell thickness of approximately 60 μm. The microparticles were spherical with smooth exterior surface. Cross-sectioning the microparticles revealed a double-layered structure (Fig. 1b). Figure 1c shows the particle size distribution in the form of a histogram. The Raman mapping result (Fig. 1d) showed that the shell and core were PLLA- and PLGA-abundant regions, respectively.

Fabrication Parameters Affecting the Size of Double-Layered Particles

By increasing stirring speed to 2000 rpm and PVA concentration to 6% (w/v), particle size was reduced to approximately 18.3 ± 4.8 μm (Figs. 2a and 2b) and the particle surface remained nonporous. The increase in stirring speed provides stronger shear forces, breaking emulsion droplets into smaller sizes, which are stabilized by the increased PVA (as a surfactant) concentration.[28] However, the cross-sectional view of the particles revealed no distinctive double-layered structure (Fig. 2c). This observation reinforces the fact that when the nascent emulsion droplets were significantly reduced, a rapid diffusion of DCM into the surrounding aqueous phase due to the higher surface area-to-volume ratio and shorter diffusion distance would occur, leading to a faster precipitation of the polymers, as reported by Katou et al.[29] At this very high polymer precipitation rate, the polymers inside the emulsion droplets do not have enough time and mobility to migrate to their respective phases to form the core–shell structure.

In order to achieve a core–shell structure for spherical particles (smaller than 10 μm) (Figs. 3a and 3b), the oil-to-water ratio was increased and the external aqueous phase was saturated with DCM. The rationale of changing these parameters is to extend the time for the polymers to coalesce with their respective polymer phases and form the double-layered structure. To clearly observe the internal structure of particles (smaller than 10 μm) and the encapsulation ability of the particles, rhodamine 6G and coumarin-6 dyes were added to the oil phase during fabrication process. The PLGA (core)–PLLA (shell) structure is shown in the confocal laser scanning microscopy CLSM image (Fig. 3c), as revealed from the color distribution of the hydrophobic coumarin-6 (green dye) in the hydrophobic PLLA shell and the hydrophilic rhodamine 6G (red dye) in the PLGA core. The preferential localization of different dyes in different polymer layers was due to the polymer–dye affinity.[4,7,12] Another characterization method, FIB, was utilized to further ascertain the internal morphology of these particles. FIB image (Fig. 3d) again shows the double-layered structure. Furthermore, a structure with bright ring and dark core was observed for the degraded particles (after 90 days *in vitro*) under FESEM fitted with a TED under dark field mode. This FESEM (with TED) image (Fig. 3e) reveals the hollow core structure within the degraded

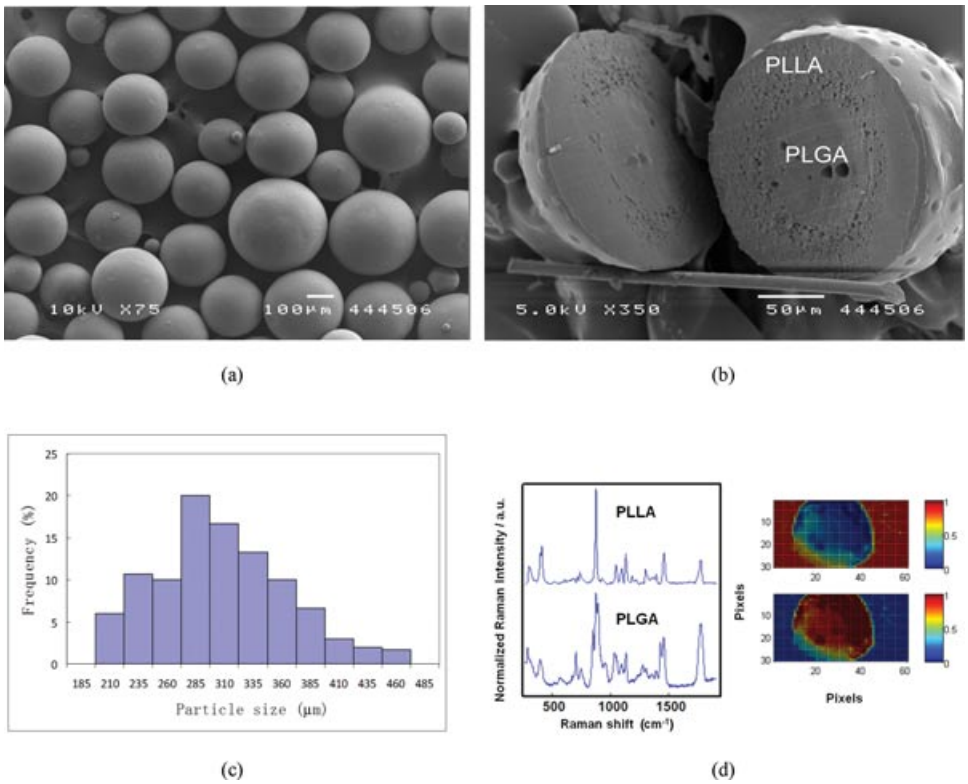

Figure 1. Large-sized double-layered PLLA/PLGA microparticles. SEM micrographs of (a) surface view of microparticles and (b) cross-sectional view of a whole microparticle. (c) Particle size distribution histogram. (d) Pure component Raman spectra estimates and their associated score images obtained via BTEM.

particles, arising from the complete erosion of PLGA core (PLGA 50:50 is known to completely degrade within 2 months),[30] leaving behind the PLLA shell. As such, the CLSM, FIB, and FESEM images affirm the formation of double-layered PLLA (shell)/PLGA (core) particles in few micron size ranges.

During the solvent removal process, DCM must diffuse into the aqueous phase before evaporating. The solubility of DCM in water is about 2% (v/v).[31] An extended solvent extraction time was required to form the double-layered particles (1–10 µm in the investigated study), which can be done by increasing the oil-to-water ratio and saturating the external aqueous phase with DCM. As a result, a decreased diffusion rate of DCM from the emulsion droplets to the external aqueous phase provided more time for the polymer coacervate droplets to coalesce with their respective phases. At the same time, the average particle size was further decreased to 2.3 µm with average shell thickness of approximately 0.6 µm. It had been reported that the increasing viscosity of the dispersed droplets during the solvent extraction process affects the droplet size equilibrium during the emulsification.[32,33] The slow precipitation rate, and thus the corresponding extended time for DCM to be extracted would then reduce the probability of nascent emulsion droplets to coalesce and agglomerate during the early step of the emulsification, thereby giving rise to the decreased particle size.

Morphological Properties of MCA-Loaded Double-Layered Particles

MCA-loaded double-layered PLLA/PLGA microparticles of different sizes were fabricated and their particle size distribution histograms are shown in Figure 4. It is to be noted that the size distribution for each of the MCA-loaded double-layered particle group did not overlap with each other, as shown in Figure 4. The sizes of these particle samples are as such: 286.5 ± 63.2 µm, 68.4 ± 24.7 µm, 17.6 ± 6.5 µm, and 2.2 ± 0.9 µm. The particles were spherical and exhibited nonporous surface. The physical characteristics of the various batches of particles (particle size, mean thickness of the shell, and calculated surface area-to-volume ratio) are shown in Table 3. The Raman mapping result (Fig. 5) showed that the core and shell comprised PLGA and PLLA, respectively, for the double-layered microparticles. Hydrophilic MCA was selectively localized in the relatively more hydrophilic PLGA core. It was observed that the layer localization of drug remains unchanged for various particle sizes.

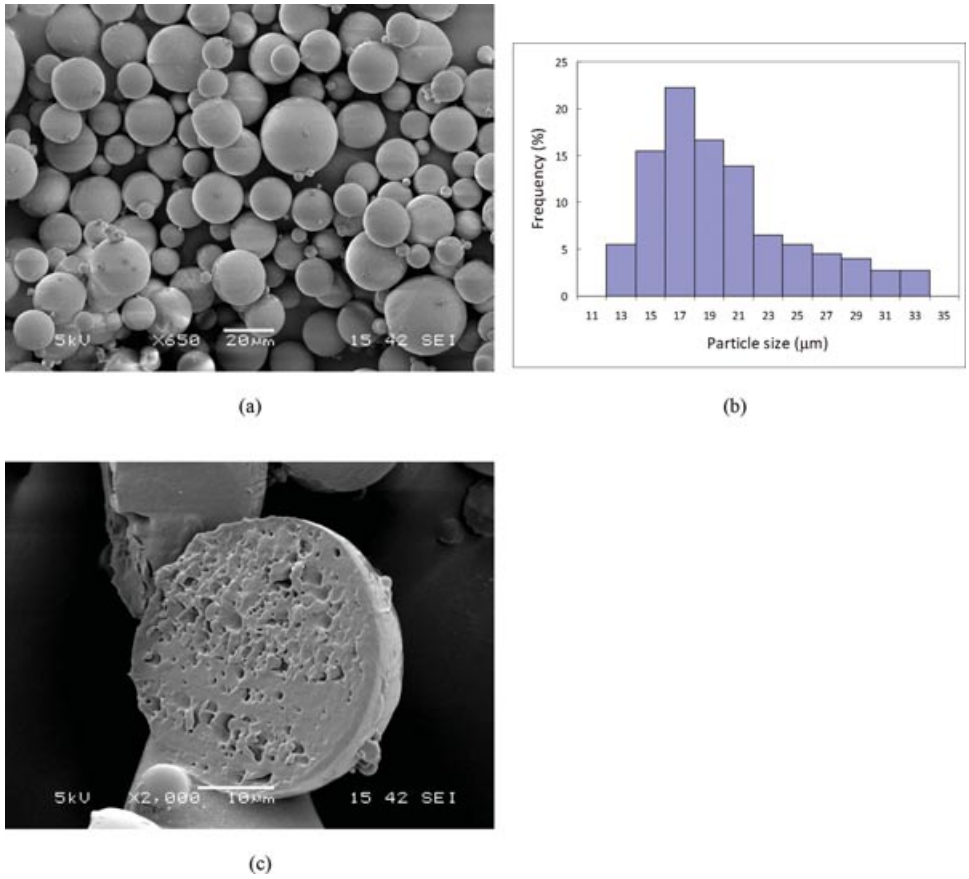

Figure 2. SEM micrographs of PLLA/PLGA microparticles. (a) Surface view of microparticles. (b) Particle size distribution histogram. (c) Cross-sectional view of a whole microparticle.

Table 3. The Physical Characteristics of the Various Batches of Particles

Particle Size (μm)	Average Shell Thickness (μm)	Calculated Surface Area-to-Volume Ratio (μm^{-1})
286.5 ± 63.2	42	0.01
68.4 ± 24.7	10	0.04
17.6 ± 6.5	2.5	0.17
2.2 ± 0.9	0.5	1.4

In Vitro Drug Release

The effects of the sizes on MCA release from the double-layered microparticles were investigated. The encapsulation efficiency of drug decreased with decreasing particle sizes. For example, loading efficiency of 53.4% was observed for particle size of 286.5 ± 63.2 μm, whereas the particles of 17.6 ± 6.5 μm exhibited the loading efficiency of 25%. This can be attributed to the fact that the small nascent emulsion droplets, giving rise to small microparticles, resulted in a short diffusion distance and a large surface area per unit mass for MCA to leach out during fabrication process.

Figure 6a plots the release profiles of MCA from the microparticles of various sizes. There was a huge initial burst (90%) of MCA from the single-layered PLGA microparticles (~28 μm). Comparatively, the PLLA shell of double-layered microparticles effectively suppressed the high initial burst release of MCA from the PLGA core. The particles of size 68.4 ± 24.7 μm was observed to exhibit slower drug release in comparison to particles of 286.5 ± 63.2 μm. The double-layered microparticles of 68.4 ± 24.7 μm exhibited a lag in MCA release up till day 14, before the drug was subsequently released. This release profile can be described as a time-delayed release.

On the contrary, the release of MCA from particles of 17.6 ± 6.5 μm and 2.2 ± 0.9 μm was faster than that from the microparticles of larger sizes (286.5 ± 63.2 μm and 68.4 ± 24.7 μm). Moreover, particles of 17.6 ± 6.5 μm and 2.2 ± 0.9 μm had relatively substantial burst release at day 1. The huge initial burst release could be attributed to the high surface area-to-volume ratio of small-sized particles (0.17 μm^{-1} for 17.6 ± 6.5 μm particles and 1.4 μm^{-1} for 2.2 ± 0.9 μm particles, as compared with 0.01 μm^{-1} for 286.5 ± 63.2 μm and 0.04 μm^{-1} for 68.4 ± 24.7 μm particles).

3% drug loading (50%), 1.5% drug loading (25%)

 DOI 10.1002/jps

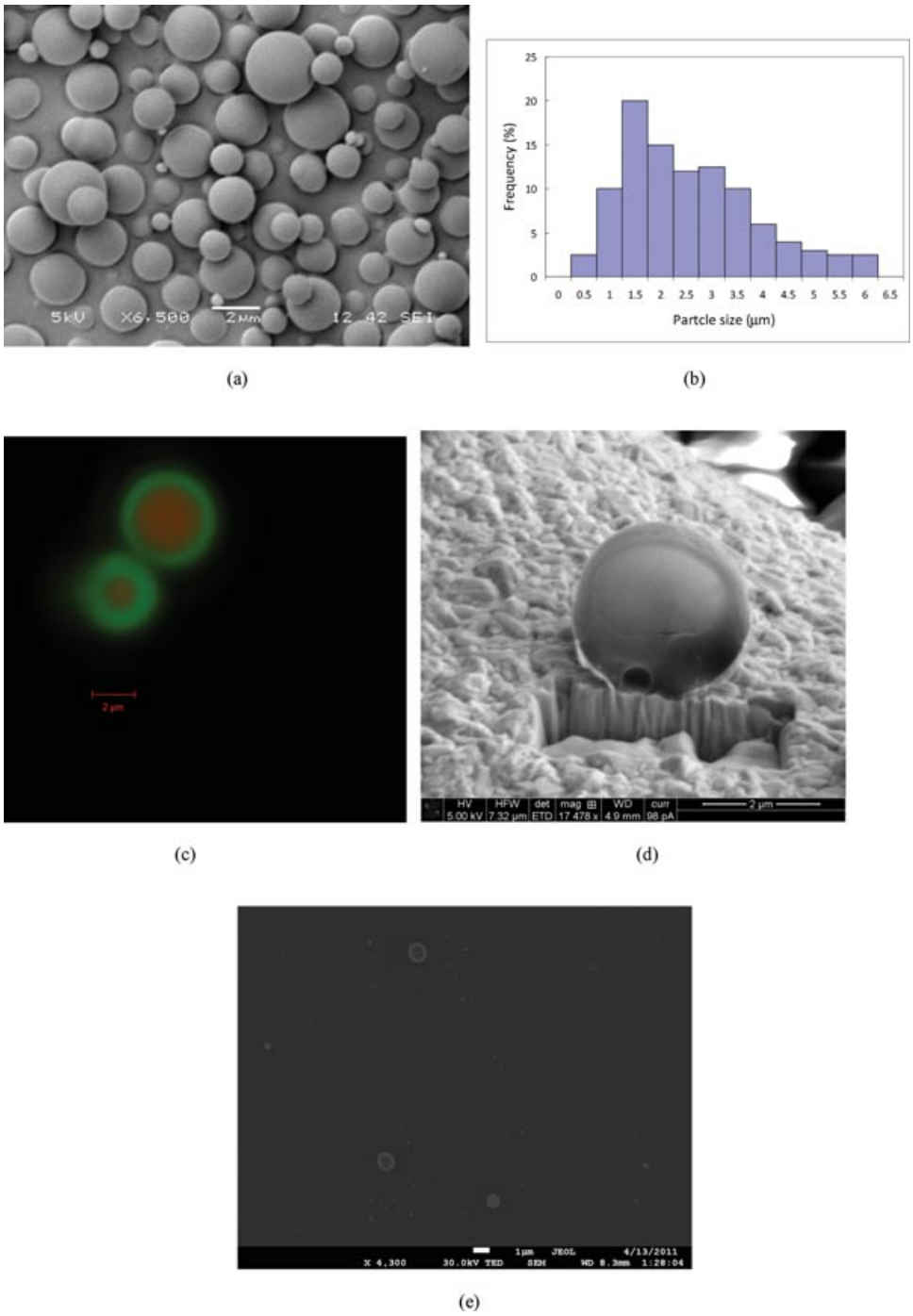

Figure 3. (a) SEM, (b) particle size distribution histogram, (c) CLSM, (d) FIB, and (e) FESEM (fitted with TED) images of double-layered PLLA/PLGA particles in few micron size ranges.

More accessible surface area would allow for MCA to diffuse into the releasing medium.

The use of double-layered particles with controllable particle sizes (ranging from several hundred microns to few microns) would be an important step toward a robust approach in controlling drug delivery kinetics. The shell can act as a rate-limiting barrier that reduces burst release of drugs. Double-layered particles can also provide pulstaile drug release kinetics for vaccination and local tumor therapy, in which a single dosage form provides an initial dose of drug followed by release-free time interval, after which second dose of drug is released. The amount of drug released in the initial and second stages can be controlled by varying particle sizes (e.g., $286.5 \pm 63.2\,\mu m$, $68.4 \pm 24.7\,\mu m$, and $17.6 \pm 6.5\,\mu m$). Furthermore, time-delayed release (i.e., the release of drug after a lag time) can be obtained for double-layered

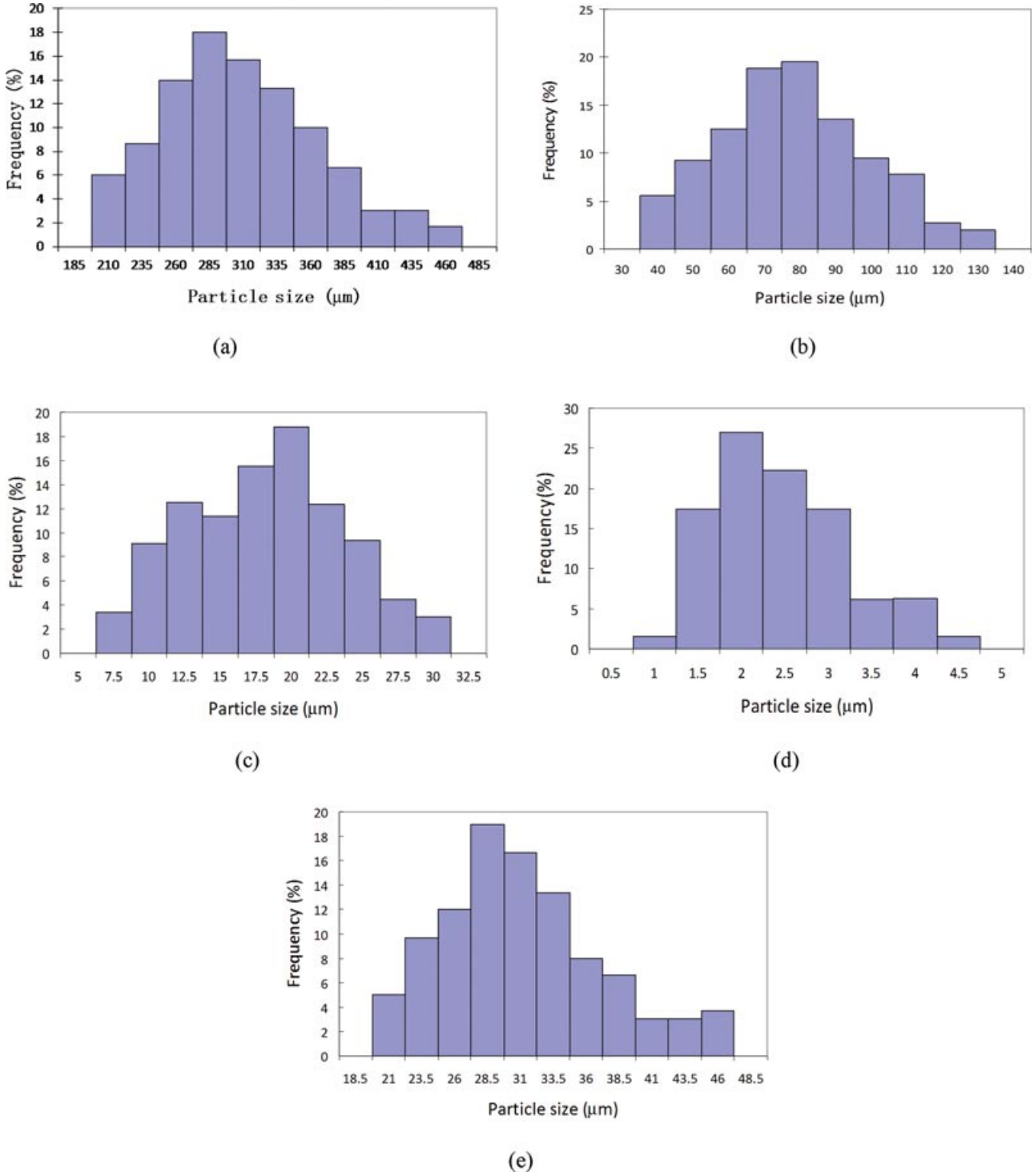

Figure 4. Particle size distribution histograms of MCA-loaded particles of sizes (a) 286.5 ± 63.2 μm, (b) 68.4 ± 24.7 μm, (c) 17.6 ± 6.5 μm, (d) 2.2 ± 0.9 μm, and (e) 28.1 ± 6.3 μm.

microparticles of 68.4 ± 24.7 μm as demonstrated in the study. This would be beneficial for drugs that have a high first-pass effect, drugs administered for diseases with chronopharmacological behavior, and cases where lag time dosing is required.

Hydrolytic Degradation of Microparticles

The drug release profile can be explained by hydrolytic degradation of the particles. As reported, the particles of 68.4 ± 24.7 μm exhibited slower drug release rates, as compared with particles of

 DOI 10.1002/jps

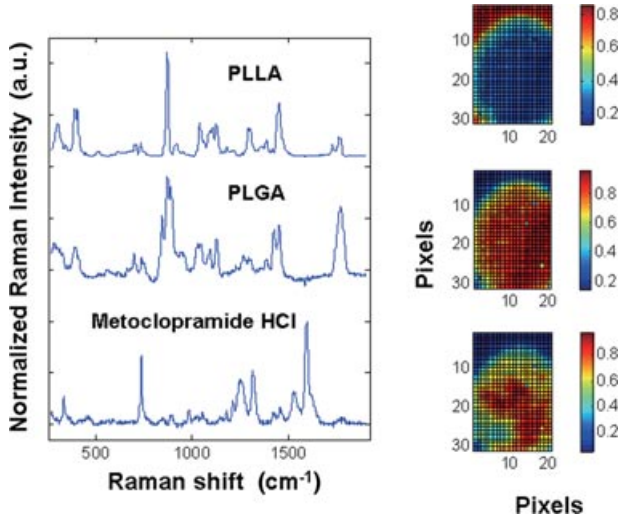

Figure 5. Pure component Raman spectra estimates and their associated score images obtained via BTEM of a MCA-loaded double-layered PLLA/PLGA microparticle.

286.5 ± 63.2 μm. This result can be explained by the significantly decreased degradation rate of the rate-limiting PLLA shell of 68.4 ± 24.7 μm, as evident from the SEC, DSC, and SEM results (Figs. 6b, 6c, and 7). This decreased degradation rate was possibly due to the fact that the shorter diffusion length with decreasing particle size would allow the acidic degradation products to diffuse out more easily into the bulk fluid.[19] Consequently, degradation of PLLA and PLGA could not be accelerated by these acidic oligomers. On the contrary, the migration of the acidic PLGA degradation products to the PLLA layer may accelerate hydrolysis of the thicker PLLA shell (average shell thickness of ~42 μm for 286.5 ± 63.2 μm particles) due to longer residence time of the acidic degradation products, as compared with 68.4 ± 24.7 μm particles with average shell thickness of approximately 10 μm.[24] In the DSC result (Fig. 6c), PLGA of the particles (286.5 ± 63.2 μm) was not detectable at day 14, which is consistent with the extensive erosion of PLGA (Fig. 7b) [while the PLGA core still remained intact at day 4 (Fig. 7a)], showing more rapid PLGA degradation for the particles (286.5 ± 63.2 μm) as compared with the particles (68.4 ± 24.7 μm). Cross-sectional views (Figs. 7c and 7d) of particles of 68.4 ± 24.7 μm show that the MCA-loaded PLGA core and PLLA shell still remained relatively intact at days 4 and 14, and thus retarding the release of MCA. The significant erosion of the PLGA core in the particles occurred after 18 days, along with the increased formation of pores in the degrading PLLA shell (Fig. 7e), which accelerated the diffusion of MCA from the core.

As can be seen in the SEC results (Fig. 6b), the decreasing rate of molecular weight of PLLA was slower with decreasing particle sizes over incubation time due to autocatalysis. However, MCA release from the particles of 17.6 ± 6.5 and 2.2 ± 0.9 μm proceeded relatively faster in comparison to the microparticles of larger sizes (286.5 ± 63.2 μm and 68.4 ± 24.7 μm). Although the autocatalytic effects were less pronounced in the smaller microparticles, the polymer degradations were not significantly

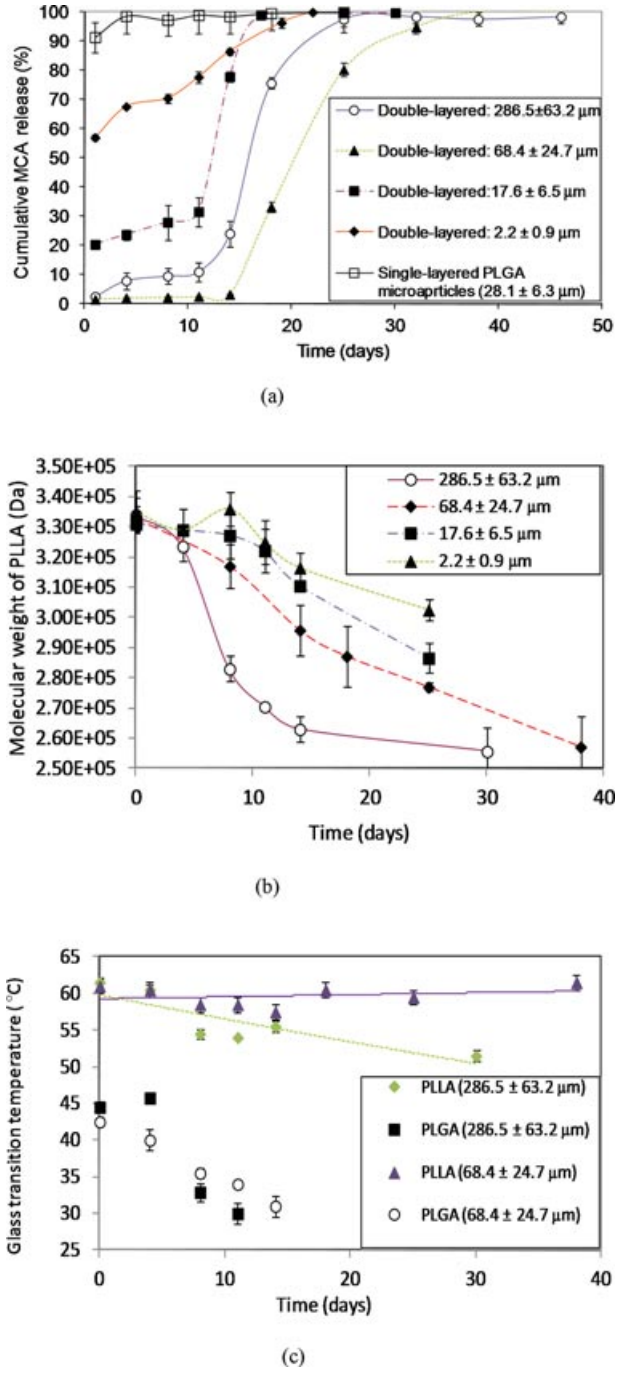

Figure 6. (a) MCA release profiles of microparticles of various sizes. (b) Changes in molecular weight of PLLA in microparticles of various sizes as a function of incubation time. (c) Change in glass transition temperatures of PLGA and PLLA in microparticles of various sizes as a function of incubation time.

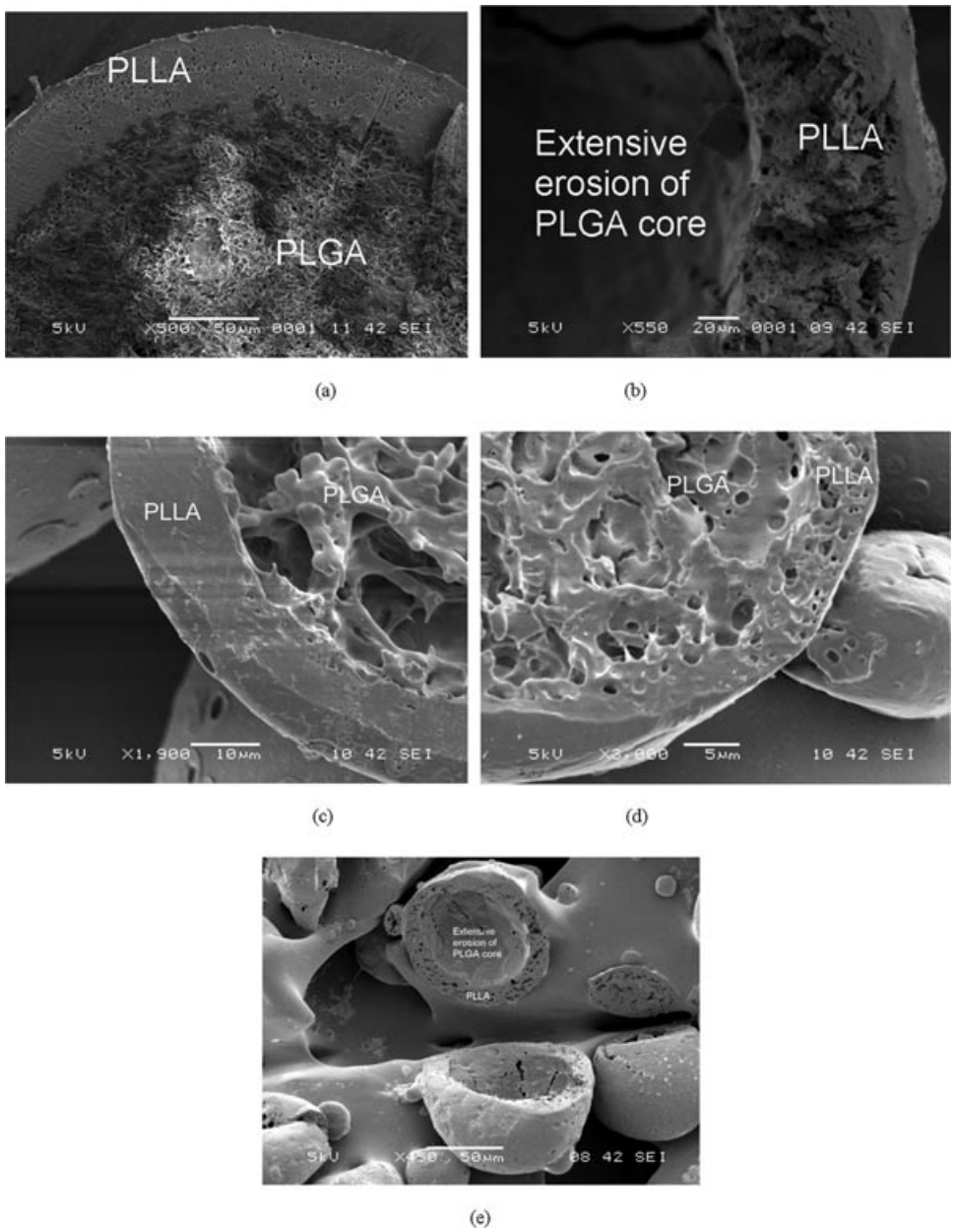

Figure 7. SEM images of the degrading MCA-loaded double-layered PLLA/PLGA microparticles. Particles of 286.5 ± 63.2 µm after (a) 4 days and (b) 14 days *in vitro*. Particles of 68.4 ± 24.7 µm after (c) 4 days, (d) 14 days, and (e) 18 days *in vitro*.

suppressed in the small-sized double-layered particles, as shown in Fig. 6b. As such, within this particle size range (around 2–20 µm), the effect of degradation rates was overcompensated by the effects of increased surface area-to-volume ratio and decreased diffusion pathway lengths with decreasing system dimension (Table 3), thus resulting in increasing drug release rate with decreasing particle size.

CONCLUSIONS

Double-layered microparticles, composed of PLGA core and PLLA shell, were fabricated using a one-step emulsion solvent evaporation technique. Increasing stirring speed and PVA concentration decreased particle sizes. When the particles size was further reduced to 2 µm, increasing the oil-to-water ratio and saturating the external aqueous phase with DCM were required to achieve the double-layered structure. By decreasing particles sizes from 286.5 ± 63.2 µm to 68.4 ± 24.7 µm, the drug release rates decreased due to slower degradation rates. However, drug release rates increased for particles in the size range of 2–20 µm, as a result of drastically increased surface area-to-volume ratios. These results provide important insights into how various double-layered

particle sizes can be achieved, and how their physical dimensions can affect drug release kinetics.

ACKNOWLEDGMENTS

The authors would like to thank the National Medical Research Council (NMRC/EDG/0062/2009 and IRG10may017) and A*STAR (project no: 102 129 0098) for the funding support in this work. The authors would also like to thank Assistant Professor Huang Yizhong and Mr. Liu Hai for the work on the FIB, and Mr. Lim Ming Pin Alan for his technical assistance in FESEM.

REFERENCES

1. Freiberg S, Zhu X. 2004. Polymer microspheres for controlled drug release. Int J Pharm 282(1–2):1–18.
2. Lu Y, Chen SC. 2004. Micro and nano-fabrication of biodegradable polymers for drug delivery. Adv Drug Deliv Rev 56(11):1621–1633.
3. Jalil R, Nixon JR. 1990. Microencapsulation using poly(L-lactic acid) IV: Release properties of microcapsules containing phenobarbitone. J Microencapsul 7(1):53–66.
4. Lee TH, Wang JJ, Wang CH. 2002. Double-walled microspheres for the sustained release of a highly water soluble drug: Characterization and irradiation studies. J Control Release 83(3):437–452.
5. Rahman NA, Mathiowitz E. 2004. Localization of bovine serum albumin in double-walled microspheres. J Control Release 94(1):163–175.
6. Kokai LE, Tan H, Jhunjhunwala S, Little SR, Frank JW, Marra KG. 2010. Protein bioactivity and polymer orientation is affected by stabilizer incorporation for double-walled microspheres. J Control Release 141(2):168–176.
7. Shi M, Yang YY, Chaw CS, Goh SH, Moochhala SM, Ng S, Heller J. 2003. Double walled POE/PLGA microspheres: Encapsulation of water-soluble and water-insoluble proteins and their release properties. J Control Release 89(2):167–177.
8. Naraharisetti PK, Ning Lew MD, Fu YC, Lee DJ, Wang CH. 2005. Gentamicin-loaded discs and microspheres and their modifications: Characterization and *in vitro* release. J Control Release 102(2):345–359.
9. Sheikh Hassan A, Sapin A, Lamprecht A, Emond E, El Ghazouani F, Maincent P. 2009. Composite microparticles with *in vivo* reduction of the burst release effect. Eur J Pharm Biopharm 73(3):337–344.
10. Khung YL, Lee WL, Chui KL, Liu Y, Lim MP, Huang CL, Loo SCJ. 2012. Microencapsulation of dye- and drug-loaded particles for imaging and controlled release of multiple drugs. Adv Healthcare Mater 1:159–163.
11. Lee WL, Loei C, Widjaja E, Loo SCJ. 2011. Altering the drug release profiles of double-layered ternary-phase microparticles. J Control Release 151:229–238.
12. Tan EC, Lin RY, Wang CH. 2005. Fabrication of double-walled microspheres for the sustained release of doxorubicin. J Colloid Interface Sci 291(1):135–143.
13. Lee WL, Yu P, Hong M, Widjaja E, Loo SCJ. 2012. Designing multilayered particulate systems for tunable drug release profiles. Acta Biomater [Epub ahead of print.]
14. Schoubben A, Blasi P, Giovagnoli S, Perioli L, Rossi C, Ricci M. 2009. Novel composite microparticles for protein stabilization and delivery. Eur J Pharm Sci 36(2–3):226–234.
15. Berkland C, Pollauf E, Pack DW, Kim K. 2004. Uniform double-walled polymer microspheres of controllable shell thickness. J Control Release 96(1):101–111.
16. Dass CR, Burton MA. 1999. Microsphere-mediated targeted gene therapy of solid tumors. Drug Deliv 6(4):243–252.
17. Philipson K, Falk R, Svartengren M, Jarvis N, Bailey M, Bergmann R, Hofmann W, Camner P. 2000. Does lung retention of inhaled particles depend on their geometric diameter? Exp Lung Res 26(6):437–455.
18. Berkland C, Cox A, Kim K, Pack DW. 2004. Three-month, zero-order piroxicam release from monodispersed double-walled microspheres of controlled shell thickness. J Biomed Mater Res 70A(4):576–584.
19. Klose D, Siepmann F, Elkharraz K, Siepmann J. 2008. PLGA-based drug delivery systems: Importance of the type of drug and device geometry. Int J Pharm 354(1–2):95–103.
20. Lee WL, Foo WL, Widjaja E, Loo SCJ. 2010. Manipulation of process parameters to achieve different ternary-phase microparticle configurations. Acta Biomater 6:1342–1352.
21. Wang Y, Guo BH, Wan X, Xu J, Wang X, Zhang YP. 2009. Janus-like polymer particles prepared via internal phase separation from emulsified polymer/oil droplets. Polymer 50(14):3361–3369.
22. Yavagal DR, Karnad DR, Oak JL. 2000. Metoclopramide for preventing pneumonia in critically ill patients receiving enteral tube feeding: A randomized controlled trial. Crit Care Med 28(5):1408–1411.
23. Lee WL, Widjaja E, Loo SCJ. 2010. One-step fabrication of triple-layered polymeric microparticles with layer localization of drugs as a novel drug-delivery system. Small 6:1003–1011.
24. Lee WL, Hong M, Widjaja E, Loo SCJ. 2010. Formation and degradation of biodegradable triple-layered microparticles. Macromol Rapid Commun 31:1193–1200.
25. Chen JL, Yeh MK, Chiang CH. 2004. The mechanism of surface-indented protein-loaded PLGA microparticle formation: The effects of salt (NaCl) on the solidification process. J Microencapsul 21(8):877–888.
26. Yeh MK, Chen JL, Chiang CH. 2002. Vibrio cholerae-loaded poly(DL-lactide-co-glycolide) microparticles. J Microencapsul 19(2):203–212.
27. Widjaja E, Lee WL, Loo SCJ. 2010. Application of Raman microscopy to biodegradable double-walled microspheres. Anal Chem 82:1277–1282.
28. Freitas S, Merkle HP, Gander B. 2005. Microencapsulation by solvent extraction/evaporation: Reviewing the state of the art of microsphere preparation process technology. J Control Release 102(2):313–332.
29. Katou H, Wandrey AJ, Gander B. 2008. Kinetics of solvent extraction/evaporation process for PLGA microparticle fabrication. Int J Pharm 364(1):45–53.
30. Visscher GE, Robison RL, Maulding HV, Fong JW, Pearson JE, Argentieri GJ. 1985. Biodegradation of and tissue reaction to 50:50 poly(DL-lactide-co-glycolide) microcapsules. J Biomed Mater Res 19(3):349–365.
31. Mao SR, Shi Y, Li L, Xu J, Schaper A, Kissel T. 2008. Effects of process and formulation parameters on characteristics and internal morphology of poly(D,L-lactide-co-glycolide) microspheres formed by the solvent evaporation method. Eur J Pharm Biopharm 68(2):214–223.
32. Mainardes RM, Evangelista RC. 2005. PLGA nanoparticles containing praziquantel: Effect of formulation variables on size distribution. Int J Pharm 290(1–2):137–144.
33. Rosca ID, Watari F, Uo M. 2004. Microparticle formation and its mechanism in single and double emulsion solvent evaporation. J Control Release 99(2):271–280.